



# Assessing the multi-decadal shoreline dynamics along the Purba Medinipur-Balasore coastal stretch, India by integrating remote sensing and statistical methods

SK Ariful Hossain<sup>1</sup> · Ismail Mondal<sup>1,2</sup> · Sandeep Thakur<sup>2</sup> · Nguyen Thi Thuy Linh<sup>3</sup> · Duong Tran Anh<sup>4</sup>

Received: 28 August 2021 / Accepted: 16 April 2022 / Published online: 23 May 2022

© The Author(s) under exclusive licence to Institute of Geophysics, Polish Academy of Sciences & Polish Academy of Sciences 2022

## Abstract

Monitoring decadal shoreline change is essential to understand the influence of coastal processes on the coastline. The shoreline is constantly shaped by natural and anthropogenic factors, and so, it is critical to understand decadal trends. The prediction of future shoreline positions is a must for effective long-term coastal zone management. This study was conducted along a 90-km-stretch of the coastline from the mouth of the Haldi River (Purba Medinipur) in the Northeast to the Subarnarekha estuary (Balasore) in the Southwest. The primary objectives of the study were to analyze the decadal shoreline migration using the End Point Rate (EPR) method and then predict future shoreline change prediction using the Kalman Filter method. Shoreline positions were digitized after extracting the shorelines using Principal Component Analysis (PCA) from Multi-temporal (1990, 2000, 2010, and 2020) and Multisensor (Landsat TM, ETM+, and OLI) satellite data. A total of 887 transects were cast to compute change statistics of the time series shoreline. It was observed that the average shoreline change rate was  $-8.41$  m/year in the periods of 1990–2000 and 2000–2010, and  $-8.80$  m/year from 2010 to 2020. Accretion along this coastal stretch is caused by the growth of morphological features such as sand bars, beaches, and dunes. We also found that erosion occurred from 1990 to 2000 along the coastline of Bhograi, Ramnagar-I, Ramnagar-II, a few parts of Contai-I, Khejuri-I, and the Nandigram-I coastal block. Accretion mostly occurred due to Land reclamation in the Northern portion of Bhograi, Contai-1 blocks and Nandigram- I block from 2000 to 2010 and 2010 to 2020. Root mean square error (RMSE) and Regression Coefficient values were computed for the future shoreline prediction of 2031 and 2041. The calculated RMSE value of  $\pm 4.7$  m and value of 0.97 shows a good relationship between the actual and predicted coastline of 2020. This study concludes that the coastline of Purba Medinipur-Balasore experienced severe erosion and needs management action and also proves the efficiency of the Digital Shoreline Analysis System (DSAS) tool for decadal analysis and prediction of shoreline change. The findings of this study may help the coastal planners, environmentalists, and coastal managers in preparing both short-term and long-term coastal zone management plans.

**Keywords** Shoreline change · Digital shoreline analysis system · End point rate · Linear regression rate · Kalman filter

Edited by Dr. Achilleas Samaras (ASSOCIATE EDITOR) / Prof. Savka Dineva (CO-EDITOR-IN-CHIEF).

✉ Duong Tran Anh  
ta.duong@hutech.edu.vn

<sup>1</sup> School of Oceanographic Studies, Jadavpur University, Kolkata 700032, India

<sup>2</sup> Department of Marine Science, University of Calcutta, Kolkata, West Bengal, India

<sup>3</sup> Institute of Applied Technology, Thu Dau Mot University, Binh Duong Province, Vietnam

<sup>4</sup> HUTECH University, 475A, Dien Bien Phu, Ward 25, Binh Thanh District, Ho Chi Minh City, Vietnam

## Introduction

The Coastline is a highly dynamic linear feature shaped by coastal processes, climate variabilities, and also human intervention (Pajak and Leatherman 2002; Maiti and Bhattacharya 2009; Cui and Li 2011). These processes continuously configure the coastline, either by erosion or accretion (Orford et al. 2002; Cooper et al. 2004; Forbes et al. 2004; Mondal et al. 2014). It is subject to numerous short-and long-term changes due to various coastal processes i.e., waves, currents, and tides, hydrodynamic changes e.g., riverine cycles and sea-level rise (Mondal et al. 2021a, b), morphological changes (e.g., formation of dune and spit

development), land-use change other factors such as rapid and seismic events (Scott 2005). Coastal erosion is a major environmental threat, mainly in the low-lying coastal regions of the world, and is a severe concern to coastal developers (Crowell et al. 1991). Erosion is the negative movement of the land because of the reduction of sediment, while accretion is the positive movement of the land due to the deposition of sediment (Mills et al. 2005). It is estimated that continuous coastal erosion has a negative impact on the livelihoods of coastal populations (Mukhopadhyay et al. 2018). Coastal erosion is responsible for the loss of inhabitable land, mangrove forests, agricultural land, and other natural and anthropogenic resources in the coastal region (Mondal et al. 2020). The complex nature of the shoreline makes it difficult to understand how much land is eroded or deposited (Fenster et al. 2001).

Erosion control is an important aspect of Integrated Coastal Zone Management, and estimation of future shoreline positions is a necessity for coastal risk reduction. To predict future shoreline position, accurate information about current and past shoreline positions are essential. Researchers (Fenster et al. 1993; Dolan et al. 1991) from across the world have successfully employed various statistical methods such as Average of Rates (AOR), End Point Rate (EPR), Linear Regression (LRR), and the Jackknife methods for the prediction of future shoreline positions. Nandi et al. (2016) used the EPR method for long-term shoreline prediction and the LRR method for short-term shoreline prediction of Sagar Island. The EPR approach forecasts shoreline position based on historical rates of shoreline change statistics whereas the LRR method predicts future shorelines based on the long-term shoreline data using a robust linear prediction method (Mondal et al. 2020). Prediction of future shoreline positions depends on many factors, like accurate delineation of the shoreline, the time of data acquisition, the number of shoreline position sample points collected from the field, and tidal conditions (Nandi et al. 2016; Mondal et al. 2020). Authors such as Li et al. (2001), Paul (2002), Srivastava et al. (2005), Purkait (2009), Chand and Acharya (2010), Kuleli (2010), Gopinath (2010), Mahapatra et al. (2018) have used the EPR and LRR method for the quantification of shoreline movement and its prediction in the last two decades. Ciritci et al. (2020) have analyzed the shoreline changes of the Izmit Gulf and Goksu Delta and predicted future shorelines positions using the Kalman filter method. In their study, they evaluated the accuracy of the model by statistical methods such as the root mean square error, correlation coefficient, and  $R^2$  value. Their research highlighted that Linear Regression and Weighted Linear Regression provide the highest accuracy for shoreline change prediction.

Multitemporal shoreline change mapping is considered as a primary input for short-and long-term coastal monitoring and assessment. Recent technological advancements such as

automatic shoreline extraction, change detection, extraction of bathymetry and topographic information, future shoreline prediction, etc., have led to improvements in coastal morphological studies. Various researches have been conducted along the Purba Medinipur and Balasore coastline through in-situ measurements, Remote Sensing, Geographic Information System (GIS), and statistical methods. Maiti and Bhattacharya (2009) have analyzed the trend of shoreline change and predicted the future shoreline using Linear Regression in response to littoral-cell. The study found that 69% of littoral cells have low RMSE for short-term shoreline prediction. The calculated RMSE value varied from 3.09 m to 945.26 m. Santra et al. (2011) have utilized high-resolution satellite images for the prediction of the future shoreline of 2015 and 2050 of the Junput coast based on the EPR method. They calculated the uncertainty of the shoreline i.e., 19.65 m. The trend of shoreline change and its future prediction of the Balasore coastal region has been conducted by Barman et al. (2015). They have used EPR and LRR methods to predict future shoreline positions and calculated the positional error by the RMSE method. The overall RMSE value was 41.88 m. Jana et al. (2016) have conducted the same study along the Digha coastal region. They have highlighted that the coast has undergone various morphological changes due to natural and human intervention.

The study area is located on the North-Eastern coast of India and is a famous tourist hotspot. Several popular beaches are located along this coast viz. Digha, Talsari, Mandarmani, Junput. The dominant coastal processes i.e., waves and tides and climate extremes such as cyclones and sea-level rise continuously alter the coastline in the area. Therefore, accurate delineation and continuous monitoring of shoreline change are essential to put remedial measures (such as afforestation, building sea walls, and dykes) against these alterations. To address this issue, predictions of future shoreline dynamics would be very helpful for coastal land resource management. Thus, the present study was undertaken with the objective of: (a) mapping and analyzing decadal shoreline change by combining remote sensing and statistical methods in a GIS platform; (b) identifying accretion and erosion-prone areas along this coastline; (c) prediction of future shoreline position of 2031 and 2041 by using Kalman filter model and evaluating the accuracy of the model using statistical methods such as RMSE and value.

## Materials and methods

### Study area

The Purba Medinipur-Balasore coastal stretch is located on the North-Eastern side of India. Geographically, the study area is bounded by latitudes between  $21^{\circ} 30' N$  and

22° 0' 54" N and longitudes between 87° 25' E and 88° 4' 26" E. The area is bound by the Haldi River (Purba Medinipur, West Bengal) in the North-East and the Subarnarekha River (Balasore, Orissa) on in the South-West and covers a coastline length of approximately 90.2 km (Fig. 1). The major geomorphic features along this coastline are active dunes, sandy beaches, mudflats, and mangrove patches, etc. The coast belongs to low-lying coastal region with wave-dominated, active dunes, and mudflats. (Dey et al. 2005) and experiences a tidal height of 2 to 4 m (Bhattacharya et al. 2003). According to Paul (2002), the coastline was formed by very thick tertiary sediment and the major geomorphic features developed in the last 6000 years BP (Dey et al. 2005; Mondal et al. 2021a, b). The area is characterized by a tropical climate with an annual mean temperature of 28 °C and annual mean rainfall of 120 cm, respectively. The coastal tract experiences 2 to 3 cyclones per year with varying intensity (Jayappa et al. 2006). Coastal erosion is a constant threat along this coast (Maiti and Bhattacharya 2009; Santra et al. 2011; Jana et al. 2016).

## Methodology

### Data used

Multi-temporal and multi-sensor satellite data of the Landsat Series viz. Thematic Mapper (TM), Enhanced Thematic Mapper plus (ETM+), and Operation Land Imager (OLI) have been utilized in the present study. The datasets were downloaded from the USGS Earth Explorer website at an interval of 10 years from the 1990s onwards to 2020 with a similar tidal condition. The details of the dataset such as date of acquisition, path, and rows, and spatial resolution are provided in Table 1.

### Data preprocessing

After procuring the dataset, layer stacking was carried out using ERDAS Imagine 2014 software. Afterward, the radiometric correction was performed on all the bands of the images. It is a two-step process that at first involves converting the DN value to radiance and then converting the radiance to reflectance (Kundu et al. 2016). In the present study, the Landsat TM images of 1990 were considered as the base map for the whole analysis.

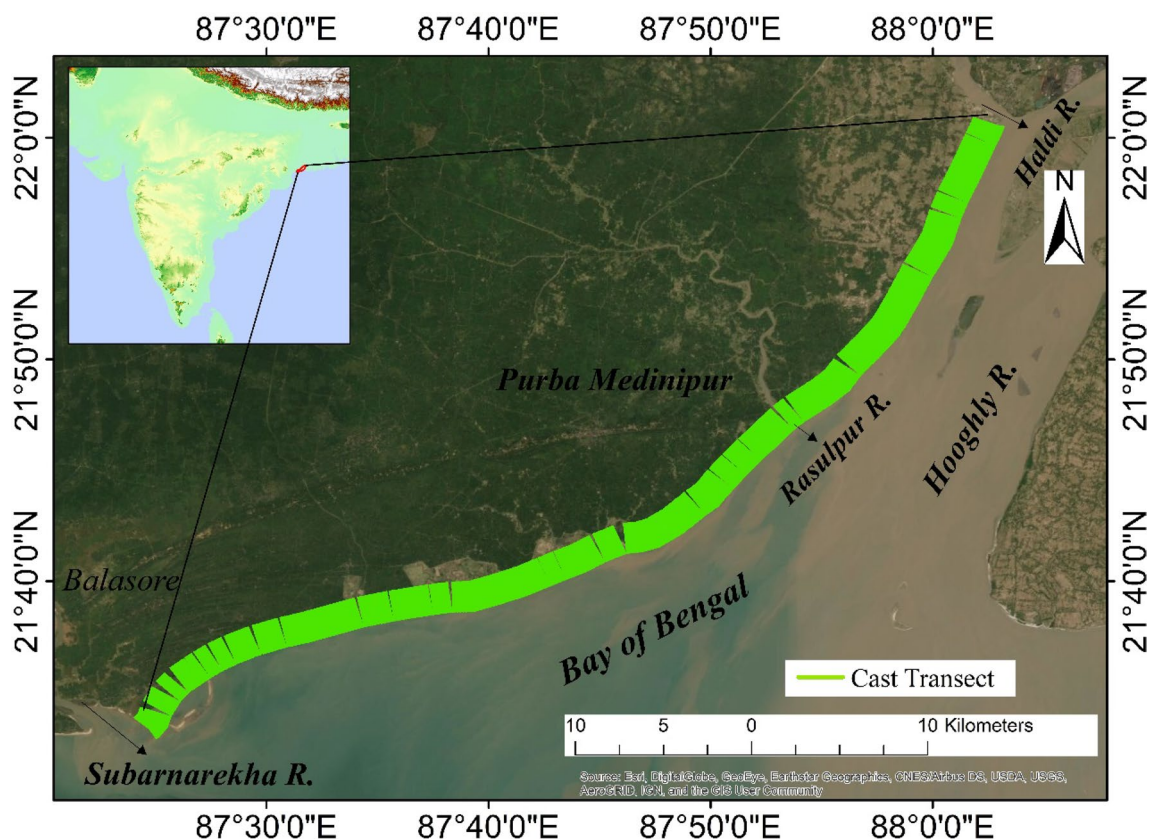


Fig. 1 Location map of the study area

**Table 1** Details of Dataset used in this study

Datasets	Path / row	Time	Resolution	Source
Landsat 4–5 Thematic Mapper (TM)	138, 139/45	January 1990, 2000	30 m	USGS Earth Explorer
Landsat 7 Enhanced Thematic Mapper+ (ETM+)	138, 139/45	January 2010	30 m	USGS Earth Explorer
Landsat 8 Operational Land Imager	138, 139/45	January 2020	30 m	USGS Earth Explorer

### Shoreline delineation

According to Pajak and Leatherman (2002), the shoreline is the high water line (HWL) on the coast however, the emergence of the water-saturated zone (Maiti and Bhattacharya 2009; Mondal et al. 2019) makes mapping the HWL very difficult. One has to take into consideration factors such as time of data acquisition and tidal condition during HWL mapping. Over the years, several image processing methods such as Normalized Difference Vegetation Index (NDVI), Tasseled Cap Transformation, Normalized Difference Water Index (NDWI), ISODATA classification, Level slicing of the SWIR band, and Principal Component Analysis (PCA) have

been used to discriminate the land water transition zone (Murali et al. 2005; Mukhopadhyay et al. 2012; Nandi et al. 2016; Mondal et al. 2016). The most successful techniques for detecting the land water transition zone are the level slicing of the SWIR band and Principal Component Analysis (Murali et al. 2005).

In the present study, shorelines were delineated by the NIR band using Principal Component Analysis (PCA) in ERDAS Imagine software (Mondal et al. 2016), and then, image segmentation techniques i.e., edge detection with  $3 \times 3$  kernels were applied to improve the contrast of the images. Afterward, the land–water transition zone was identified using visual interpretation (Fig. 2D), and shorelines

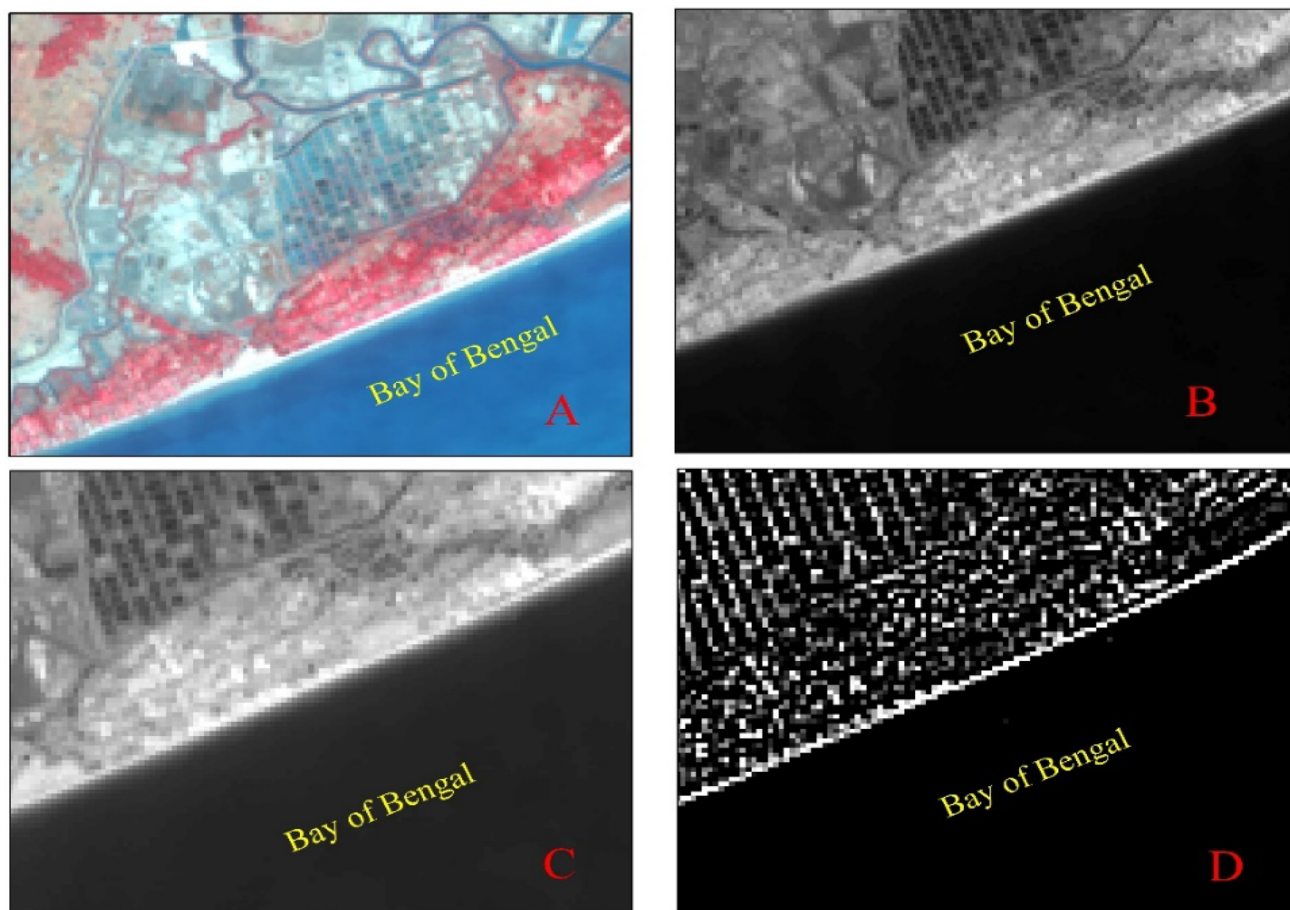


**Fig. 2** Shoreline detection: **A** Standard FCC image; **B** Original NIR Band; **C** PCA; **D** PCA with Edge Detection

were digitized using feature analysis tool in esri@Arc Map version 10.5 (Fig. 3). The necessary fields such as Object ID, shape length, and Date\_ were provided in the attribute table of the shoreline because this information is necessary during the calculation process in DSAS.

### Baseline creation and generation of the transect using Digital Shoreline Analysis System (DSAS) tool

The baseline was constructed toward the seaward side at a specific distance from the shoreline. During baseline construction, the fields such as ID and Group\_, OFFshore, and CastDir are fed to the attribute table. This information is needed to understand the transect order and baseline location relative to the shoreline during the DSAS calculation process.

Later, transects were generated at 100-m-intervals and cast perpendicular to the baseline using the DSAS tool (Fig. 4). The transect length was given 1500 m from baseline, and shoreline change statistics was computed using the EPR and LRR method in this study. With respect to baseline, regression of shoreline is known as negative movement indicating erosion, whereas progradation of shoreline is considered as positive movement, indicating accretion.

### Field survey

Field surveys were conducted for ground verifications, and ground points were collected using a Garmin GPS (precision 15 m) at various coastal sites between January 2020 and January 2021. The ground locations were surveyed using a simple random sampling method. The temporal data sets were examined over a long period (1990–2020), and future predictions were made for 2031 and 2041.

### Calculation of shoreline change rate

The EPR and LRR methods are the most popular and widely accepted by researchers and coastal planners throughout the world because of their robustness and simplicity. To run this model for shoreline change analysis, no prior information related to wave inferences, sediment transport, etc., is required (Li et al. 2001; Mondal et al. 2021a, b). In the study, estimation of the rate of decadal shoreline change has been done using the EPR model while prediction of future shoreline positions was done by LRR method. The detailed conceptual framework of the work flow is shown in Fig. 5.

done using the EPR model while prediction of future shoreline positions was done by LRR method. The detailed conceptual framework of the work flow is shown in Fig. 5.

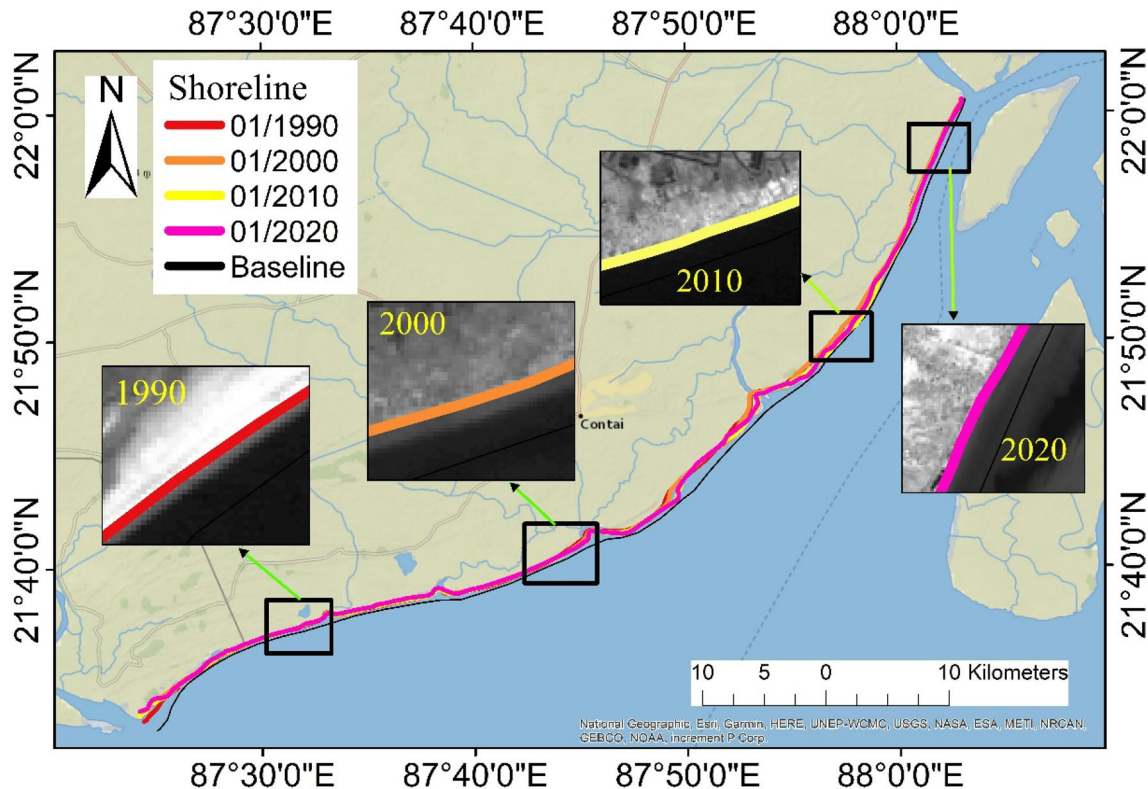
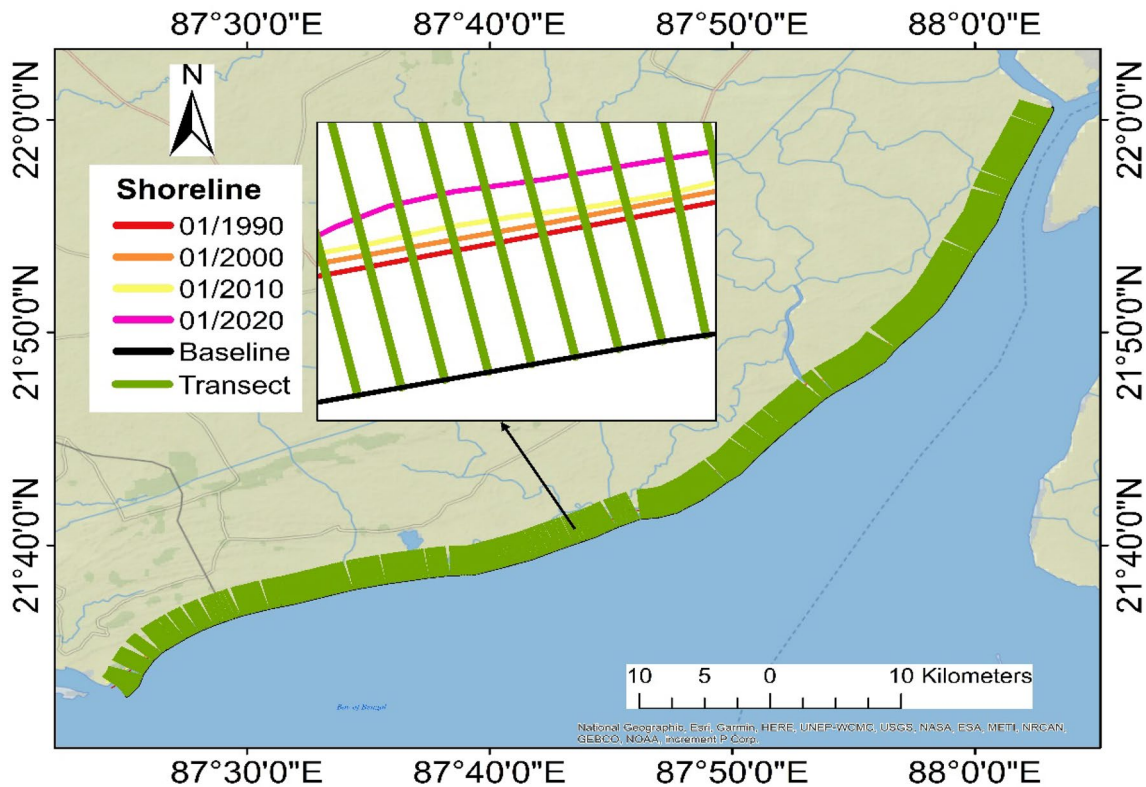


Fig. 3 Shoreline detection using PCA with edge detection of the respective year



**Fig. 4** Cast transects plotted across the shoreline from the baseline

**a. End Point Rate (EPR) method** The EPR is a statistical technique that is used to compute the shoreline change rate by dividing the distance of shoreline movement and the time intervals between the oldest and most recent shorelines. The formula of EPR is expressed in Eq. 1:

$$\text{EPR} = \frac{(D_1 - D_2)}{(t_2 - t_1)}, \quad (1)$$

where  $D_1$  is the distance of shoreline movement of the base year,  $D_2$  is the distance of shoreline movement of the current year,  $t_1$  is the oldest time, and  $t_2$  is the recent time.

**b. Linear Regression Rate (LRR) method** The LRR is a reliable statistical method that has been used by researchers all over the world to measure the rate of shoreline change and predict the future positions of the shoreline (Crowell et al. 1997; Nandi et al. 2016). In this method, the rate of shoreline change statistics is calculated by fitting the least-square regression line to all the points for a specific transect (Himmelstoss et al. 2018). It shows the relationship between the time (indicates year) and the movement of the shoreline from the baseline. The regression coefficient or sum of residual squares (value ranges from 0 to 1 (one indicating good accuracy and zero indicating no accuracy) and can be used to assess the accuracy of these methods (Maiti and

Bhattacharya 2009). The slope of the line represents the rate of change of the shoreline. It requires long-term shoreline data to compute the rate of shoreline change. Figure 6 shows that LRR value of 14 number transects i.e.,  $-33.18$  (slope).

#### Accuracy assessment and future shoreline prediction

EPR and LRR statistical methods were used to analyze the shoreline change. The RMSE value was then calculated using the following Eq. (2), which was based on the actual shoreline positions obtained from time-series satellite images and the prediction of shoreline change at the same date. Also, the regression coefficient value was calculated using a scatter plot based on the LRR output of the actual and model-derived shorelines on the same date. The Kalman Filter utilized in DSAS combines observed shoreline position with model-derived position to forecast future shoreline position. The Kalman Filter method uses the linear regression rate of past shoreline data from DSAS to predict where the shoreline would be every 10th or 20th year (Long and Plant, 2012; Himmelstoss et al. 2018). The Kalman filter is a robust and efficient statistical method widely used in coastal geophysical applications (Wilson et al. 2010). It is a predictive method that predicts the future based on historical data (Ciritci et al. 2020).

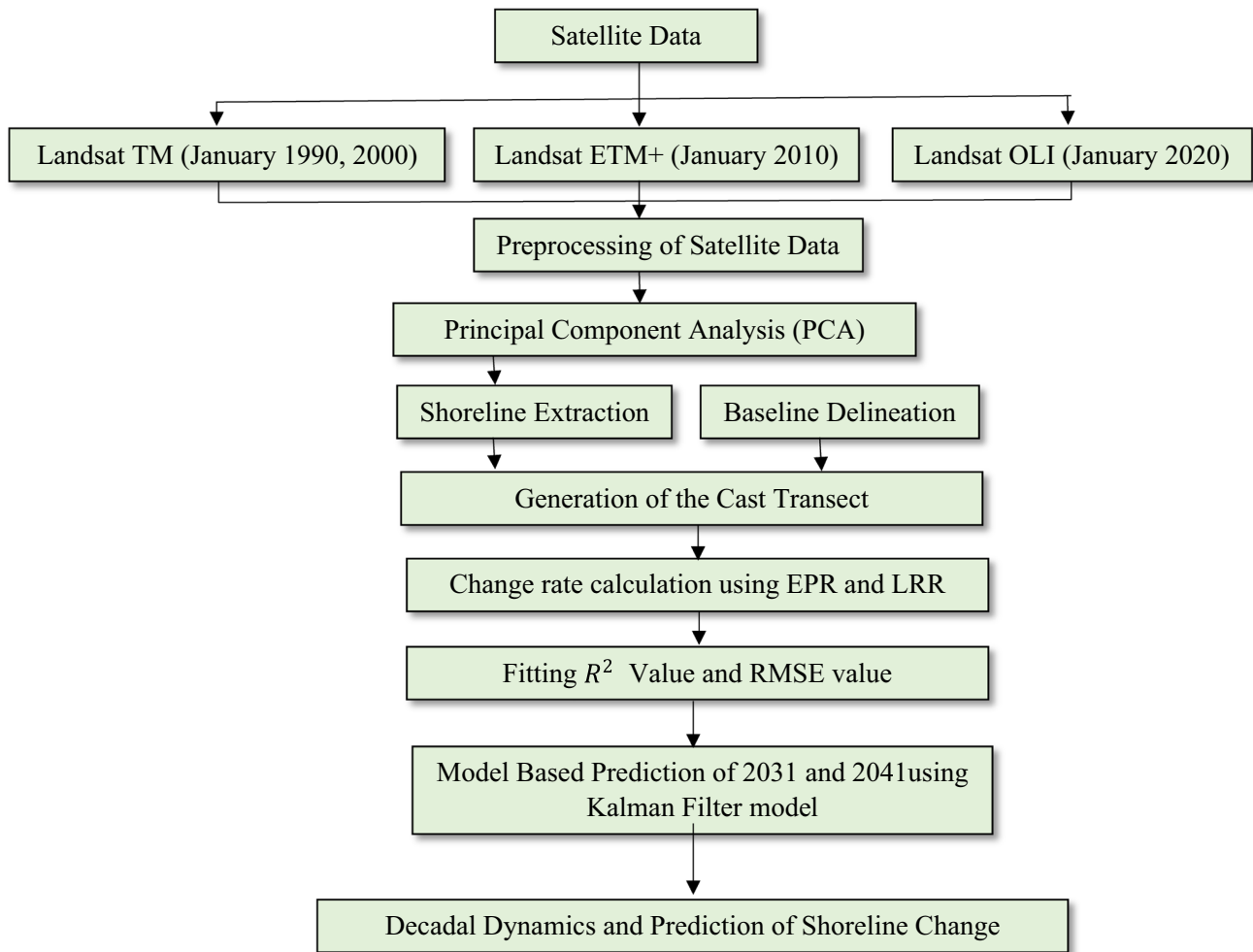


**Fig. 5** Details methodological framework for shoreline change analysis and its prediction

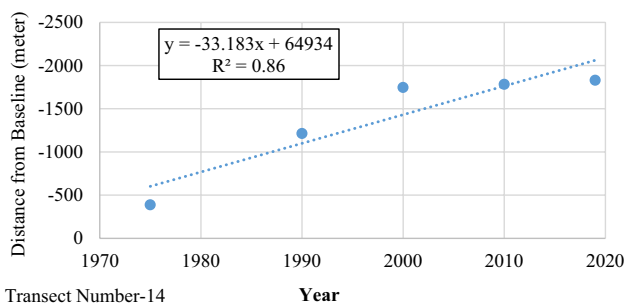


**Fig. 6** Linear Regression Rate (LRR) of shoreline change

$$\text{RMSE} = \sqrt{\{(X_{\text{mod}} - X_{\text{org}})^2 + (Y_{\text{mod}} - Y_{\text{org}})^2\}}, \quad (2)$$

where  $X_{\text{mod}}$  and  $Y_{\text{mod}}$  are the model-based shoreline position, and  $X_{\text{org}}$  and  $Y_{\text{org}}$  are the known shoreline position.

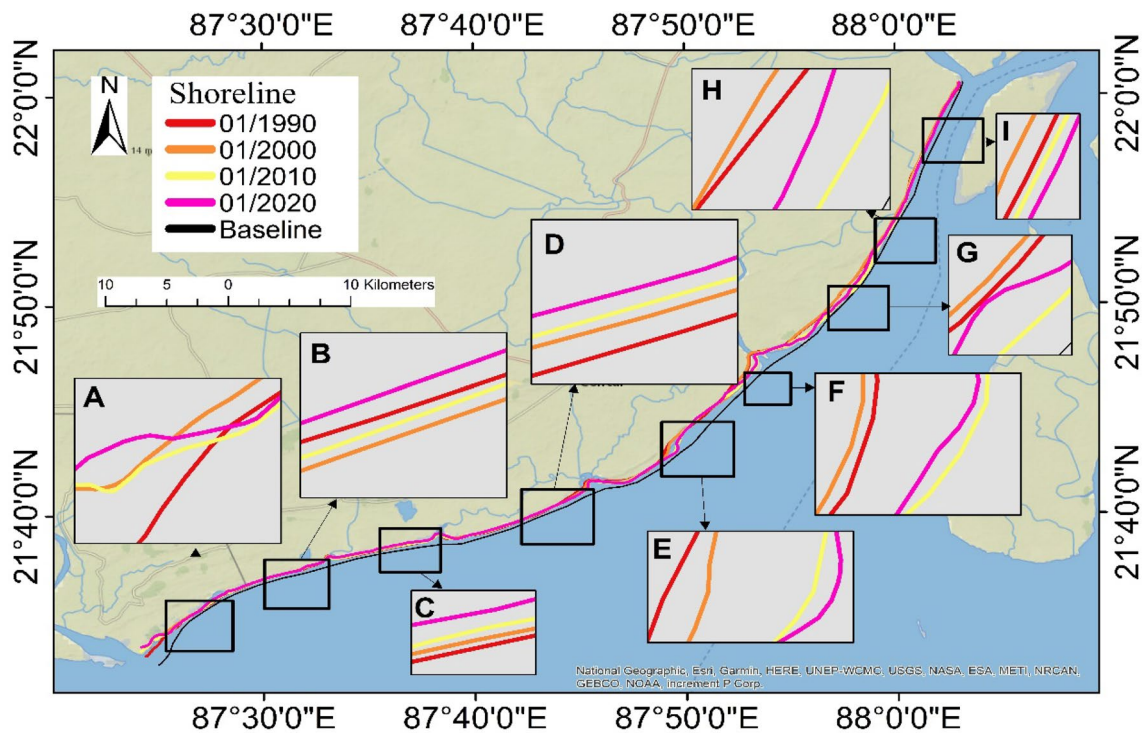
## Results and discussion

### Analysis of decadal shoreline change from 1990 to 2020

Mapping of shoreline change was carried out on the Medinipur and Balsore coastal stretches for a period of three decades viz. 1990 to 2000, 2000 to 2010, and 2010 to 2020. To estimate the rate of shoreline change, the EPR and LRR techniques were used, and the detailed statistics of decadal shoreline change are given in Table 2. The negative value represents erosion, whereas the positive value represents accretion. The decadal shoreline change maps (Fig. 7) and graphs (Fig. 8) were produced using an Arc map and an Excel sheet based on the EPR data. In the decadal change of shoreline maps, the light red to dark red color represents low to high erosion, whereas the light green to dark green color shows low to high accretion. Figure 9 shows the Spatio-temporal variability of shoreline change, showing that shoreline

**Table 2** Details statistics of decadal shoreline change from 1990 to 2020

Parameters	1990–2000	2000–2010	2010–2020
Number. of Transects	887	887	887
Number of Erosion Transects	656 (73.95%)	617 (69.56%)	638 (71.92%)
Number of Accretion Transects	231 (26.05%)	270 (30.44%)	249 (28.08%)
Number of High Erosion Transects	341 (38.44%)	346 (39.01%)	356 (40.14%)
Number of High Accretion Transects	65 (7.67%)	98 (11.05%)	33 (3.72%)
Number of Low Erosion Transects	315 (35.51%)	271 (30.55%)	282 (31.79%)
Number of Low Accretion Transects	163 (18.38%)	172 (19.39%)	216 (24.35%)
Average Erosion rate (meter/year)	− 8.41	− 8.41	− 8.80
Average Accretion rate (meter/year)	10.92	10.92	4.73
Maximum Erosion rate (meter/year)	− 66.32	− 62.73	− 41.01
Maximum Accretion Rate (meter/Year)	40.78	46.24	26.27
Minimum Erosion Rate (meter/year)	− 0.04	− 0.02	− 0.01
Minimum Accretion Rate (meter/year)	0.01	0.01	0.01

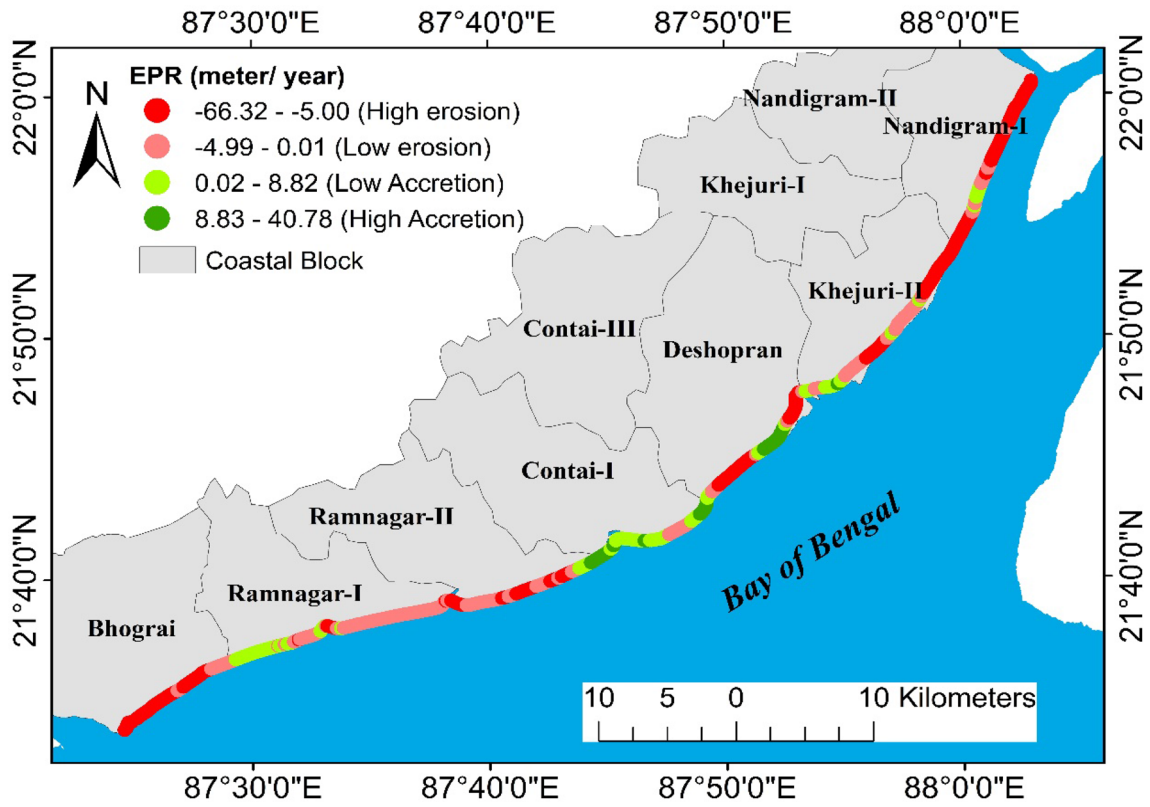
**Fig. 7** Spatio-temporal variability of Shoreline Change

change is almost linear in most of the coastal stretch due to changes in morphological characteristics such as a sand bar, dune, beaches, and mudflats.

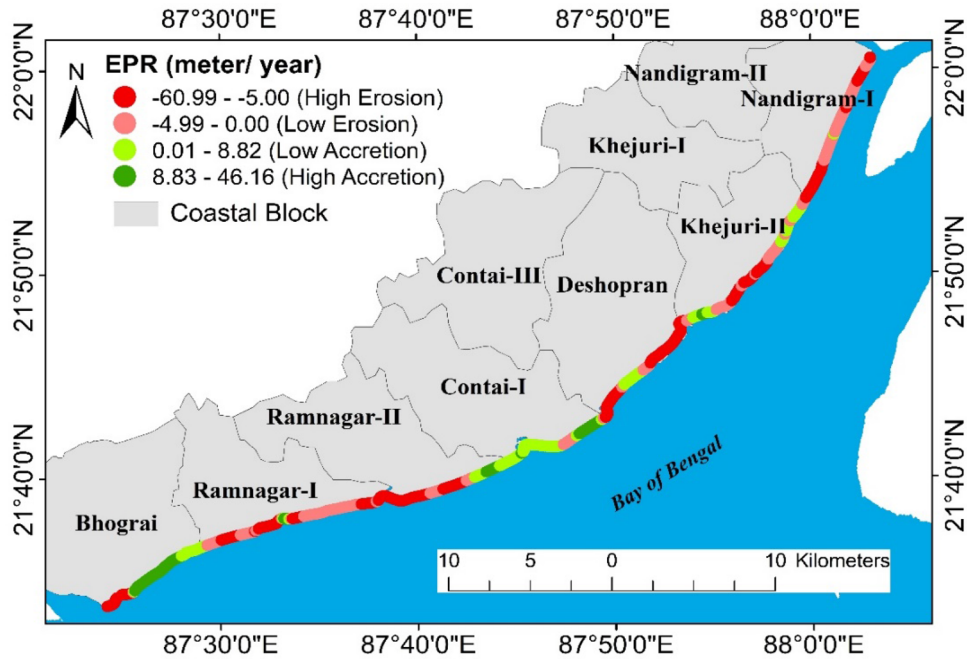
It was observed that the rate of maximum erosion was found to be  $-66.32$  m,  $-62.73$  m, and  $-41.01$  m from 1990 to 2000, 2000 to 2010, and 2010 to 2020, respectively, at the mouth of the Subarnarekha River due to the reduction of mangrove forest. The maximum accretion rate was  $40.78$  m,  $46.24$  m, and  $26.27$  m from 1990 to 2000, 2000 to 2010, and 2010 to 2020, respectively, which occurred in

the eastern part of the Contai-I block due to land reclamation. The decadal map clearly shows that low to high erosion was observed on the coastlines of Bhograi, Ramnagar-I, Ramnagar-II, and a few parts of Deshopran, Khejuri-II, and Nandigram-I block due to morphological changes by coastal processes and human intervention, while low to high accretion was observed on a few parts of the western part of Ramnagar-I and Contai-I block from 1990 to 2000 due to artificial construction. High accretion occurred on the eastern part of the Bhograi block's coastline between 2000





(a)



(b)

**Fig. 8** Decadal Shoreline Change Map based on End Point Rate (EPR) Method **a** 1990 to 2000, **b** 2000 to 2010, and **c** 2010 to 2020

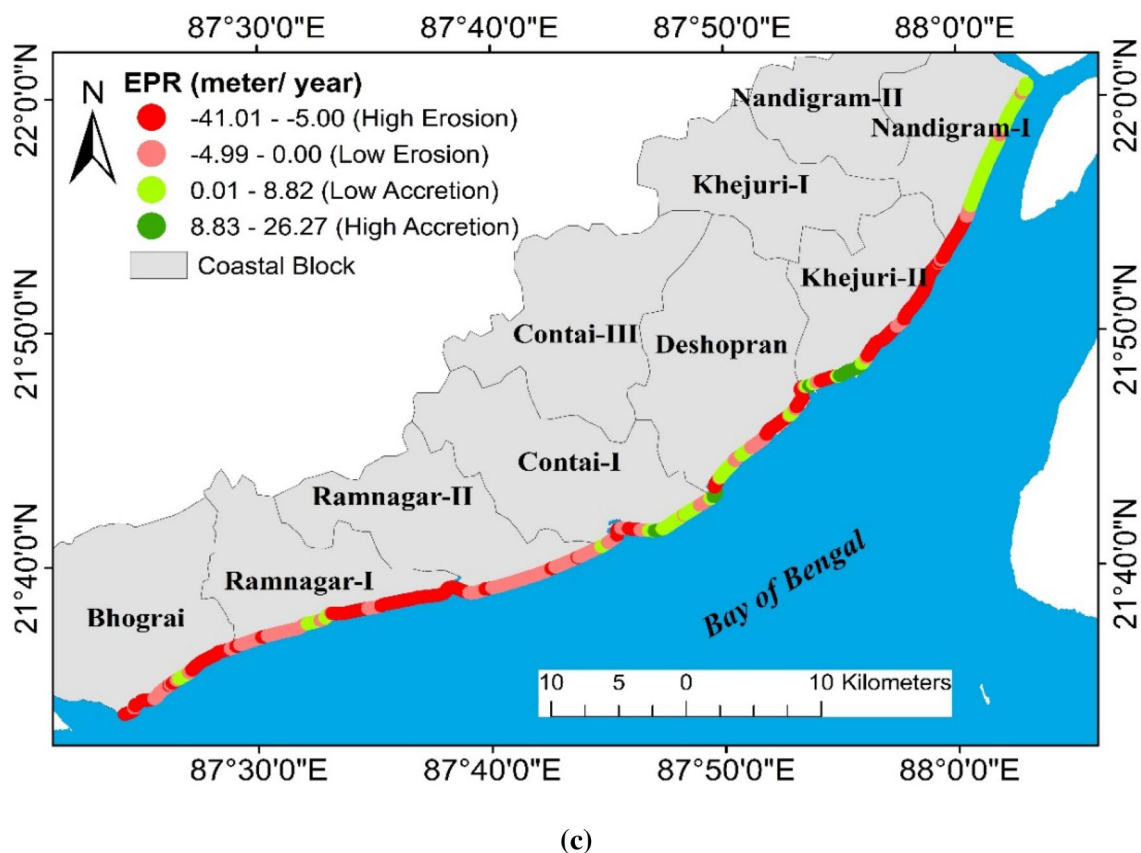


Fig. 8 (continued)

and 2010 because of the use of soft engineering techniques such as dune stabilization with casuarina tree plantations. It was observed that low accretion was found on the coastline of Nandigram-I from 2010 to 2020 due to the deposition of sediment by the river.

The decadal analysis of 1990–2000 found that 38.44% of the total coastline was under high erosion, followed by low erosion (35.51%), low accretion (18.38%), and high accretion (7.67%). Similarly, the analysis from 2000 to 2010 showed that 39.01% of the total coastline was prone to high erosion, followed by low erosion (30.55%), low accretion (19.39%), and high accretion (11.05%). According to the analysis from 2010 to 2020, high erosion occurred 40.14% of the coastline, followed by low erosion (31.79%), low accretion (24.35%), and high accretion (3.72%). Figure 10 shows an increasing trend in high erosion on the coast from 1990 to 2020, due to the combined effect of both cyclonic activity and high tide, resulting in the destruction of coastal ecosystems and a high amount of suspended material washed by river discharge. The accretion occurred on the coastline of the Contai-I block due to the implementation of the structure of the barrier and sea wall, and the placement of sandbags and gabions which have caused the deposition of sediments

and progradation of the shoreline. The study discourses that the coast was eroded continuously because of the dominant coastal processes, such as waves and tides, climatic extreme events, reduction of sediment supplied by the river, and land-use change. The coast is located on the eastern coast of India, which is frequently affected by cyclonic activities and storm surges (IMD Cyclone e-Atlas, 2011) that make the coastline more susceptible to severe erosion.

### Prediction of future shoreline of 2031 and 2041

The future shorelines of 2031 and 2041 have been predicted by the model-based Kalman Filter in the DSAS v5 tools. Based on the positional values of 1990, 2000, and 2010, the shoreline of 2020 was predicted to validate the model's accuracy. The Regression Coefficient ( $r$ ) value was then computed using a scatter plot based on the LRR output of the actual and model-derived 2020 shorelines. The calculated  $r$  value was 0.97 (Fig. 11), indicating a good relationship between the actual and predicted 2020 shorelines, and the RMSE value was calculated to validate the model output and, finally, predict the future shoreline, and the overall RMSE value was  $\pm 4.73$  m. Afterward, the

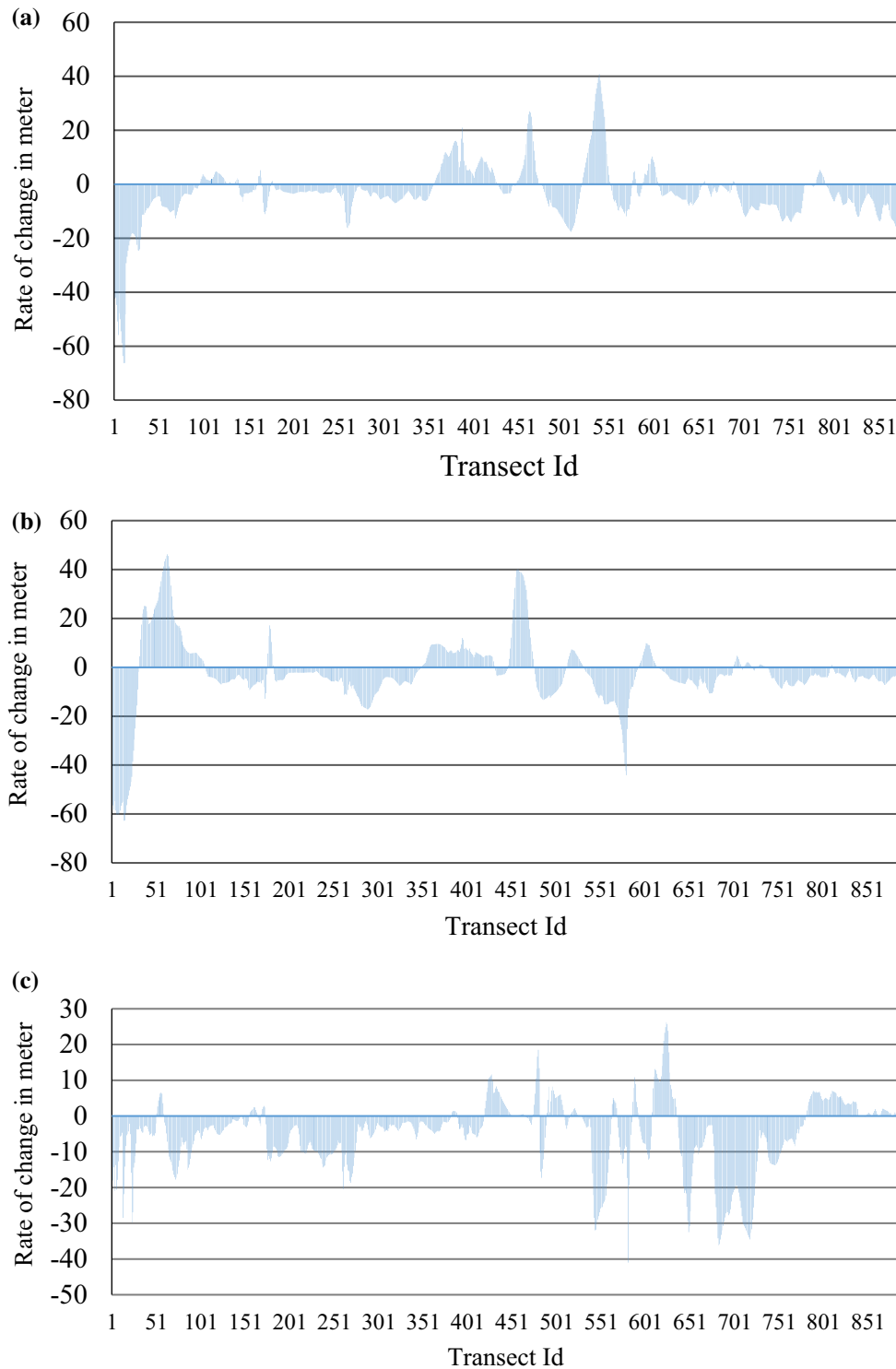


**Fig. 9** The graph shows the Decadal Shoreline Change Analysis based on EPR **a** 1990 to 2000, **b** 2000 to 2010, and **c** 2010 to 2020

model was performed for the shoreline prediction of 2031 and 2041 which is shown in Fig. 12. The results showed that erosion will occur continuously along the coastal stretches if the coastal protection measures have not been

implemented. As a result, the coastal community will face a serious problem in the future, and also it will degrade the biophysical condition of the coastal environment.



**Fig. 10** Field Photograph of Shoreline degradation and impact of ecosystem

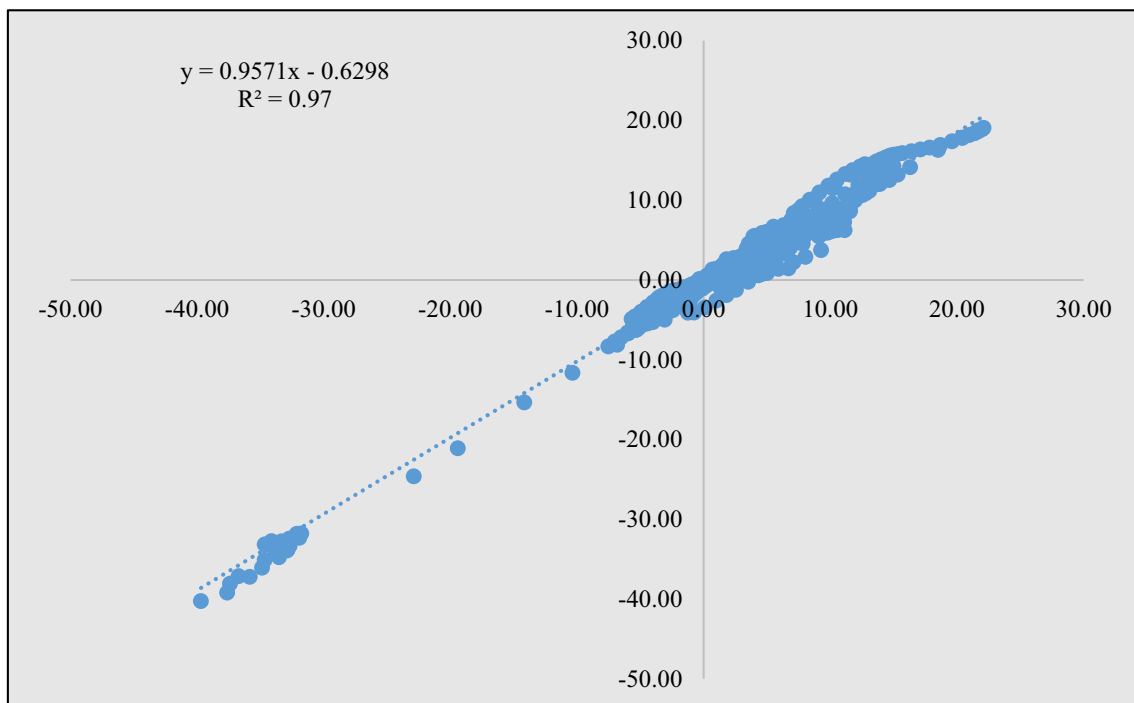


**Fig. 11** Fitting LRR for Original and Predicted shoreline of 2020

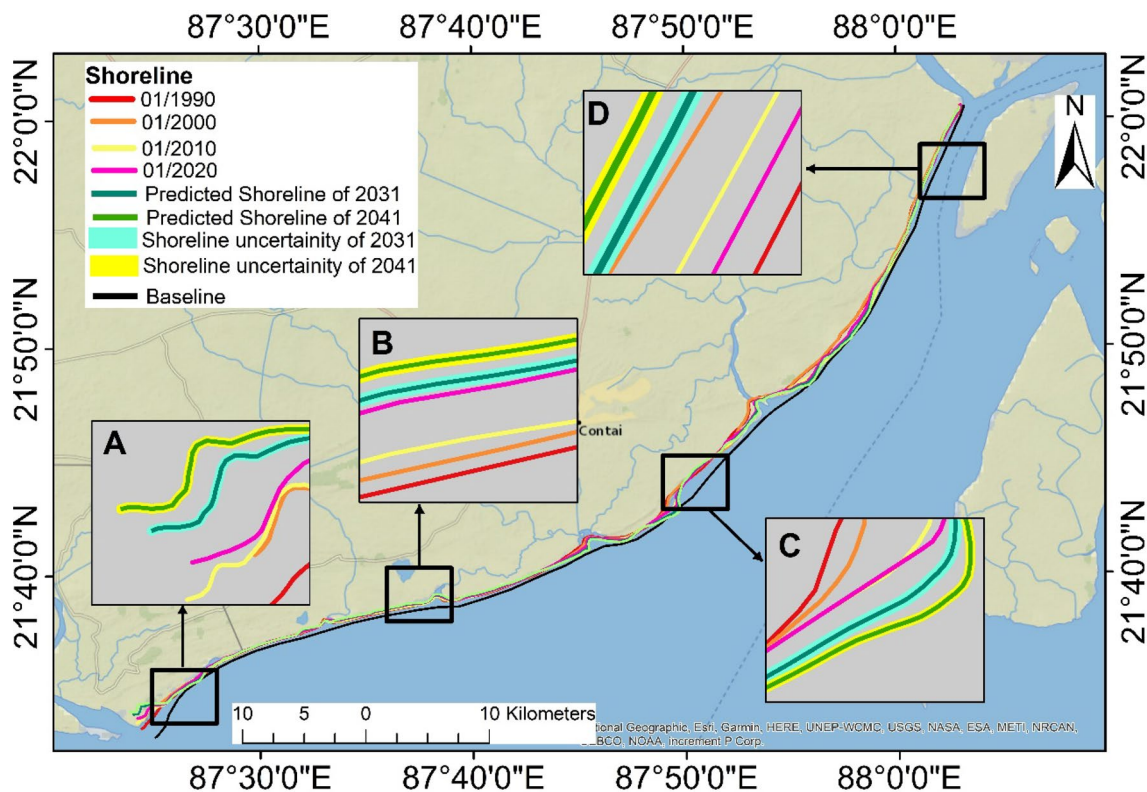


Fig. 12 Shoreline prediction of 2031 and 2041 using Kalman Filter model

## Conclusion

The quantification and prediction of shoreline changes are essential to prepare a sustainable solution for coastal risk reduction. The study concludes that this coast has experienced severe erosion over the last few decades due to natural and anthropogenic factors. To understand the complexity of the shoreline, transect-wise analysis was carried out at a decadal scale. We found that massive erosion has occurred in the coastal stretches due to frequent storm and cyclonic activities, active coastal processes, lack of sediment supply, and land-use change. The accretion has been found only in a few parts of the coastal stretch, due to artificial construction, the dumping of sandbags, and the plantation of casuarina trees. The erosion occurred in the coastal block Bhogra, Ramnagar-I, Ramnagar-II, and a few parts of Deshopran, Khejuri-II, and Nandigram-I, and accretion occurred in the coastal block of the western part of Ramnagar-I and Contai-I block.

The Kalman filter method was used to predict the future shoreline of 2031 and 2041 shows that erosion will occur along the coastal stretch if proper mitigation measures have not been implemented. This study may help coastal planners and policymakers to prevent coastal erosion and to reduce the adverse conditions which occur continuously along this

coastal stretch. Here, multi-temporal satellite data have been utilized to analyze the pattern of shoreline change and forecast the future coastline, which may aid in mitigating the damage caused by these activities. The EPR and LRR models were used for shoreline change quantification and the future shoreline prediction of 2031 and 2041. A long-term coastal zone management plan would benefit from the shoreline forecast map. The study conclusively proves the efficiency of the DSAS tool for the decadal analysis and prediction of shoreline change. Finally, we believe that more research into hydrodynamic modeling, sea-level rise, and beach profiling will help us to understand the causes of morphological change and coastal morphodynamics. The study recommends that remedial measures such as Boulder dumping, construction of embankment, placement of the geosynthetic tube, plantation of casuarina trees, and mangrove trees along this coastal stretch would be very helpful to prevent or reduce the significant adverse environmental and societal impacts on the coast.

**Acknowledgements** Sincere thanks to the University Grant Commission (UGC), Government of India for providing the fellowship to conduct this study, and also would like to thank the USGS for providing the free satellite images and DSAS tools. The authors extend their thank to the anonymous reviewer for their valuable comments and suggestion which helped us to improve this manuscript.

**Author Contributions** SAH: Conceptualization, Writing-original draft, Software, Formal analysis, Visualization, and editing. IM, ST, AMF AI-Q, and NTTL and DTA: Writing, review, editing, and suggestion.

## Declarations

**Conflict of interest** This manuscript has not been published or presented elsewhere in part or entirety and is not under consideration by another journal. There are no conflicts of interest to declare.

## References

- Barman NK, Chatterjee S, Khan A (2015) Trends of shoreline position: an approach to future prediction for Balasore Shoreline, Odisha, India. *Open J of Mari Sci* 5:13–25
- Bhattacharya A, Sarkar S K, Bhattacharya A (2003) An assessment of coastal modification in the low lying tropical coast of north east India and role of natural and artificial forcings. In: International conference on estuaries and coasts, 2003, November pp. 9–11, Hangzhou, China
- Chand P, Acharya P (2010) Shoreline change and sea level rise along coast of Bhitarkanika wildlife sanctuary, Orissa: an analytical approach of remote sensing and statistical techniques. *Int J Geomat Geosci* 1:436–454
- Chen AJ, Chen CF, Chen KS (1995) Investigation of shoreline change and migration along Wai-San-Ding-Zou barrier Island, central western Taiwan. *Geosci Remote Sens Symp* 3:2097–2099
- Ciritci D, Türk T (2020) Assessment of the Kalman filter-based future shoreline prediction method. *Int J Environ Sci Technol* 17:3801–3816. <https://doi.org/10.1007/s13762-020-02733-w>
- Cooper JA, Jackson D, Nava F, Mckenna J, Malvarez G (2004) Storm impacts on an embayed high energy coastline, Western Ireland. *Mar Geol* 210:261–280
- Crowell M, Leatherman SP, Buckley MK (1991) Historical shoreline change: error analysis and mapping accuracy. *J Coast Res* 7:839–852
- Crowell M, Douglas BC, Leatherman SP (1997) On forecasting future US shoreline positions: a test of algorithms. *J Coast Res* 13(4):1245–1255
- Cui B, Li X (2011) Coastline change of Yellow River estuary and its response to the sediment and runoff (1976–2005). *Geomorphology* 127:32–40
- Deepika B, Avinash K, Jayappa KS (2014) Shoreline change rate estimation and its forecast: remote sensing, geographical information system and statistics-based approach. *Int J Environ Sci Technol* 11(2):395–416
- Dey S, Ghosh P, Nayak A (2005) The influences of natural environment upon the evolution of sand dunes in tropical environment along Midnapur coastal area. *India Indones J Geogr* 37(1):51–68
- Dolan R, Fenster MS, Holme SJ (1991) Temporal analysis of shoreline recession and accretion. *J Coast Res* 7:723–744
- Fenster MS, Dolan R, Elder JF (1993) A new method for predicting shoreline positions from historical data. *J Coast Res* 9:147–171
- Fenster MS, Dolan R, Morton RA (2001) Coastal storms and shoreline change: signal or noise? *J Coast Res* 17:714–720
- Forbes D, Parkers G, Manson G, Ketch K (2004) Storms and shoreline retreat in the southern Gulf of St. Lawrence *Mar Geol* 210:169–204
- Gopinath G (2010) Critical coastal issues of Sagar Island, east coast of India. *Environ Monit Assess* 160:555–561
- Himmelstoss EA, Farris AS, Henderson RE, Kratzmann MG, Ergul A, Zhang O, Zichichi JL, Thieler ER (2018) Digital shoreline analysis system (version 5.0): U.S. Geological Survey software. <https://code.usgs.gov/cch/dsas/>
- IMD- Cyclone e-Atlas (2011) Tracks of cyclones and depressions over North Indian Ocean (from 1891 onwards). Cyclone Warning and Research Centre, India Meteorological Department, Regional Meteorological Centre Chennai, Version 2, 48p
- Jana A, Maiti S, Biswas A (2016) Analysis of short-term shoreline oscillations along Midnapur-Balasore Coast, Bay of Bengal, India: a study based on geospatial technology. *Model Earth Syst Environ* 2(2):64
- Jayappa KS, Mitra D, Mishra AK (2006) Coastal geomorphological and land-use and land-cover study of Sagar Island, Bay of Bengal (India) using remotely sensed data. *Int J Remote Sens* 27:3671–3682
- Kuleli T (2010) Quantitative analysis of shoreline changes at the mediterranean coast in turkey. *Environ Monit Assess* 167:387–397
- Li R, Liu JK, Felus Y (2001) Spatial modelling and analysis for shoreline change detection and coastal erosion monitoring. *Mar Geod* 24:1–12
- Long JW, Plant NG (2012) Extended Kalman Filter framework for forecasting shoreline evolution. *Geophys Res Lett* 39(1–6):L13603. <https://doi.org/10.1029/2012GL052180>
- Long M, Leatherman SP, Buckley MK (1991) Historical shoreline change error analysis. *J Coastal Res* 7:839–852
- Maiti S, Bhattacharya AK (2009) Shoreline change analysis and its application to prediction: a remote sensing and statistics based approach. *Mar Geol* 257:11–23
- Mahapatra M, Ratheesh R, Rajawat AS (2014) Shoreline Change Analysis along the Coast of South Gujarat, India, Using Digital Shoreline Analysis System. *J Indian Soc Remote Sens* 42:869–876. <https://doi.org/10.1007/s12524-013-0334-8>
- Mills JP, Buckley SJ, Mitchell HL, Clarke PJ, Edwards SJ (2005) A geomatics data integration technique for coastal change monitoring. *Earth Surf Process Landf* 30:651–664
- Mondal I, Bandyopadhyay J (2014) Coastal zone mapping through geospatial technology for resource management of Indian Sundarban. West Bengal, India. *Int J Remote Sens Appl* 4(2):103–112. <https://doi.org/10.14355/ijrsa.2014.0402.04>
- Mondal I, Thakur S (2020) Bandyopadhyay J (2019) Delineating lateral channel migration and risk zones of Ichamati River. West Bengal, India, *J Clean Prod Elsevier* 244:118740
- Mondal I, Bandyopadhyay J, Dhara S (2016) Detecting shoreline changing trends using principle component analysis in Sagar Island, West Bengal, India, *Journal of Spatial Information Research*. Springer Nature 25(1):67–73. <https://doi.org/10.1007/s41324-016-0076-0>
- Mondal I, Thakur S, Juliev M, Bandyopadhyay JD, TK. (2020) Spatio-temporal modelling of shoreline migration in Sagar Island. West Bengal, India, *J Coast Conserv Springer* 24(50):1–20. <https://doi.org/10.1007/s11852-020-00768-2>
- Mondal I, Thakur SG, De PB, T.K. (2021a) Assessing the impacts of global sea level rise (SLRR) on the mangrove forests of indian sundarbans using geospatial technology. *Geograp Inform Sci Land Resour Manag Wiley* 11:209–228. <https://doi.org/10.1002/978119786375.ch11>
- Mondal I, Thakur S, De A, Bandyopadhyay J, De TK (2021b) Estimating water quality of sundarban coastal zone area using landsat series satellite data. *River Health and Ecol South Asia (springer)*. [https://doi.org/10.1007/978-3-030-83553-8\\_8.pp.155-172](https://doi.org/10.1007/978-3-030-83553-8_8.pp.155-172)
- Mukhopadhyay A, Mukherjee S, Mukherjee S, Ghosh S, Hazra S, Mitra D (2012) Automatic shoreline detection and future prediction: a case study on Puri coast, Bay of Bengal, India. *Europe J Remote Sens* 45:201–213
- Mukhopadhyay A, Ghosh P, Chanda A, Ghosh A, Ghosh S, Das S, Ghosh T, Hazra S (2018) Threats to coastal communities of

- mahanadi delta due to imminent consequences of erosion – Present and near Future. *Sci of the Tot Environ* 637–638:717–729
- Murali Krishna G, Mitra D, Mishra AK, Oyuntuya, Sh, Nageswra Rao K (2005) Evaluation of semi-automated image processing techniques for the identification and delineation of coastal edge using IRS, LISS-III Image – A Case Study on Sagar Island, East Coast of India. *International Journal of Geoinformatics*, Vol.1, No. 2
- Nandi S, Ghosh M, Kundu A, Dutta D, Baks M (2016) Shoreline shifting and its prediction using remote sensing and GIS techniques: a case study of Sagar Island, West Bengal(India). *J Coast Conserv* 20:61–80. <https://doi.org/10.1007/s11852-015-0418-4>
- Orford JD, Forbes DL, Jennings SC (2002) Organizational controls, typologies and time scales of paraglacial gravel-dominated coastal systems. *Geomorphology* 48:51–85
- Pajak MJ, Leatherman S (2002) The high water line as shoreline indicator. *J Coast Res* 18:329–337
- Paul AK (2002) Coastal geomorphology and environment: Sundarban Coastal Plain, Kanthi Coastal Plain. ACB Publication, Kolkata, Subarnarekha Delta plain
- Purkait B (2009) Coastal erosion in response to wave dynamics operative in Sagar Island, Sundarban delta, India. *Front Earth Sci Chin* 3:21–33
- Reshma KN, Murali RM (2018) Current status and decadal growth analysis of krishna - godavari delta regions using remote sensing. *J Coastal Res* 85:1416–1420
- Santra A, Mitra D, Mitra S (2011) Spatial modeling using high resolution image for future shoreline prediction along Junput Coast, West Bengal, India. *Geo Spatial Info Sci* 14:157–163
- Scott DB (2005) Coastal changes, rapid. In: Schwartz MI (ed) *Encyclopedia of coastal sciences*. Springer, the Netherlands, pp 253–255
- Srivastava A, Niu X, Di K, Li R (2005) Shoreline modeling and erosion prediction, ASPRS 2005 Annual Conference B Geospatial Goes Global: From Your Neighborhood to the Whole Planet^ March 7– 11, 2005, Baltimore, Maryland
- Thakur S, Maity D, Mondal I, Basumatary GG, De PB, T.K. (2020a) Assessment of changes in land use, land cover, and land surface temperature in the mangrove forest of Sundarbans, northeast coast of India. *Environ Dev Sustain* 22(3):1–29. <https://doi.org/10.1007/s10668-020-00656-7>
- Thakur S, Mondal I, Bar I, Nandi S, Ghosh PB, Das P, De TK (2020b) Shoreline changes and its impact on the mangrove ecosystems of some islands of Indian Sundarbans, North-East coast of India. *J Clean Prod* ISSN 124764:0959–6526. <https://doi.org/10.1016/j.jclepro.2020.124764>
- Wilson G, Özkan-Haller H, Holman R (2010) Data assimilation and bathymetric inversion in a 2dh surf zone model. *J Geophys Res* 115:C12057. <https://doi.org/10.1029/2010JC006286>